

2.5 Results of Rainfall Distribution Analysis

2.5.1 Days when rainfall was observed

(1) August 10, 1983

The cloud brightness patterns were established for the four Wadi and Wadi Ahin separately by assuming that the cloud patterns moved toward WNW according to the general wind direction (ESE) at high altitude.

The following regression results were obtained from the established cloud brightness patterns (CCT count) and the average altitude of the rainfall observation points (436 m).

$$R = 0.391 \times C - 34.2 + 0.0435 \times (h - 436)$$

(Coefficient of correlation : 0.68)

wherein,

R : Daily rainfall (mm)

C : Digital count

h : Altitude (m)

The regression equation was applied to the subject areas. The resultant rainfall distribution image is shown in Fig. F-2-4 (1).

(2) December 29, 1984

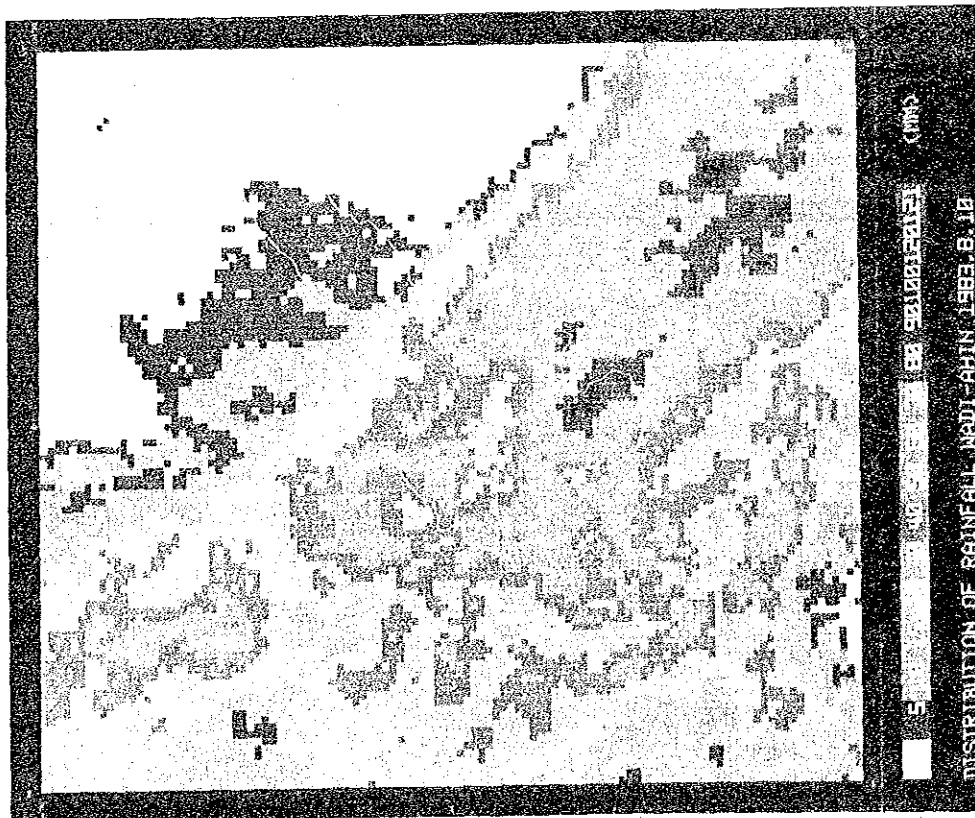
Because the rainfall concentrated in three hours around the time when the NOAA data was collected (16:00), the following regression relation was obtained from the cloud brightness distribution and the daily rainfall.

$$R = 0.743 \times C - 54.4$$

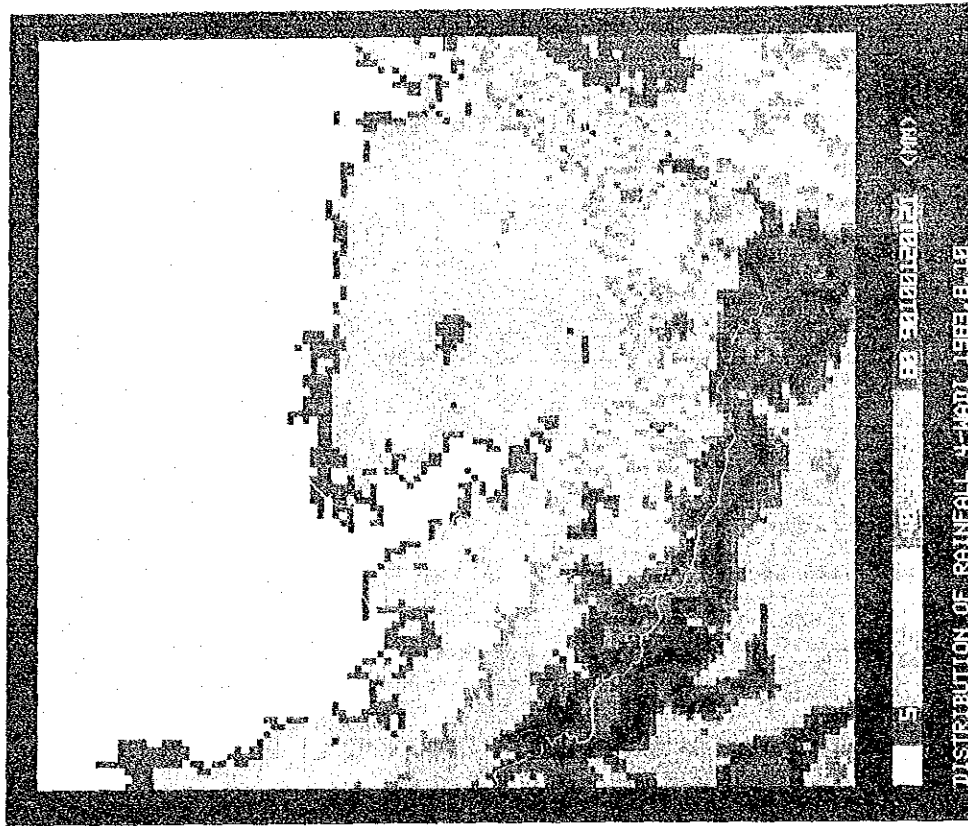
(Coefficient of correlation: 0.73)

The regression equation was applied to the subject areas. The resultant rainfall distribution image is shown in Fig. F-2-4 (2).

Fig. F-2-4(1) Precipitation Distribution Image (1/3)

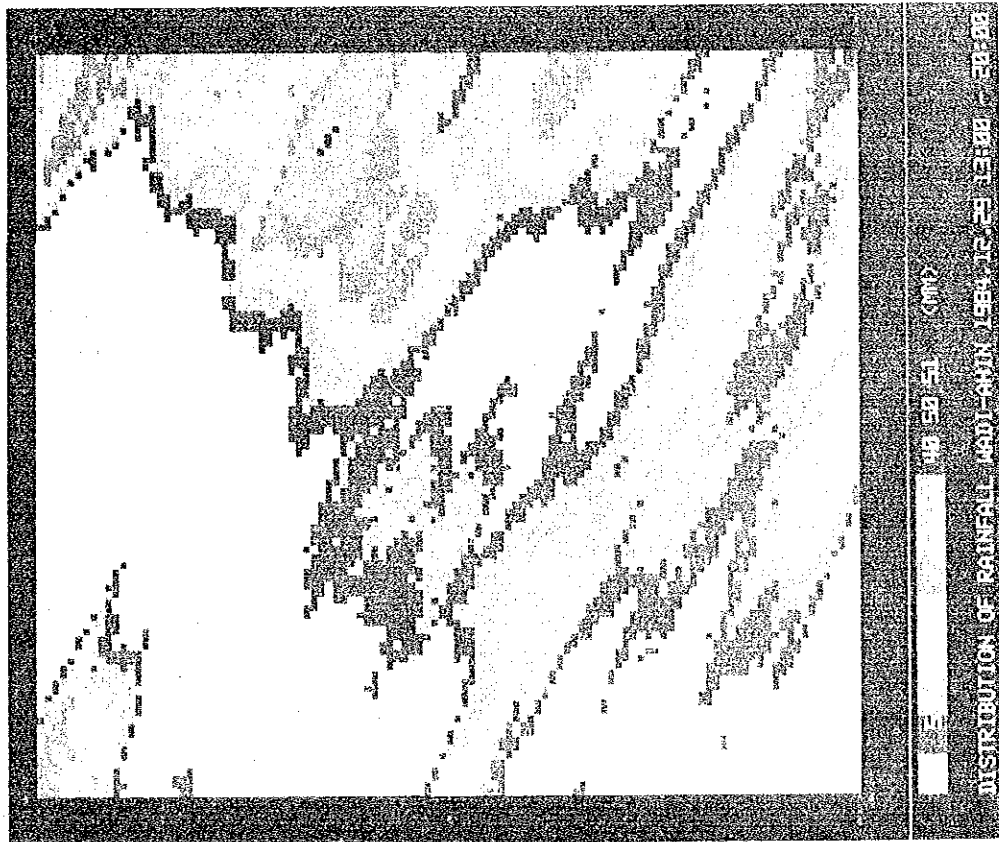


(a) Wadi Ahin Area, Aug. 10, 1984

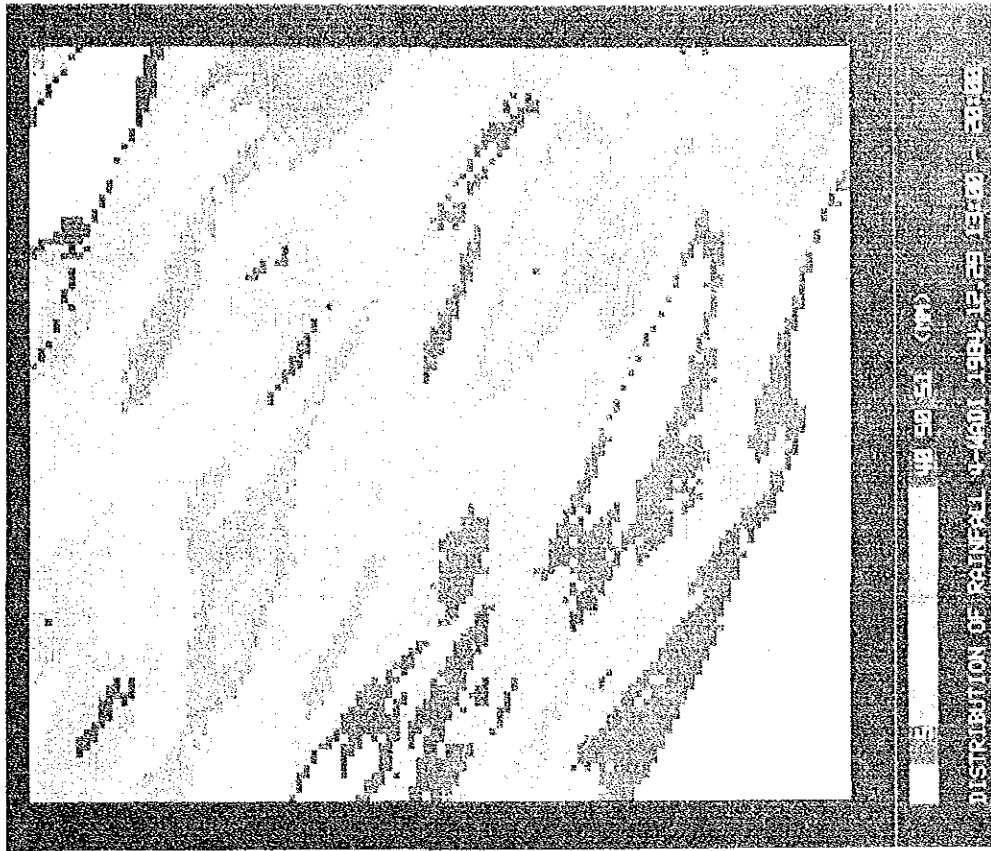


(b) 4 Wadi Area, Aug. 10, 1984

Fig. F-2-4(2) Precipitation Distribution Image (2/3)



(a) Wadi Ahin Area, Dec. 29, 1984



(b) 4 Wadi Area, Dec. 29, 1984

2.5.2 Days when rainfall was not observed or observed only at a few sites:

(1) April 13, 1983

The rainfall observation sites were limited only to MF2 and MAF. Although it was very difficult to obtain a significant regression relation from data at two points, the rainfall distribution image shown in Photo-10 was created based on general estimation from the cloud brightness patterns. (Fig. F-2-4 (3))

(2) January 7, 1985

The rainfall was limited to only three sites of RF3, RK3 and RK4 in the mountain. Although it was very difficult to obtain a significant regression relation from data at three points, the rainfall distribution image shown in Photo-11 was created based on general estimation from the cloud brightness patterns. (Fig. F-2-4 (3))

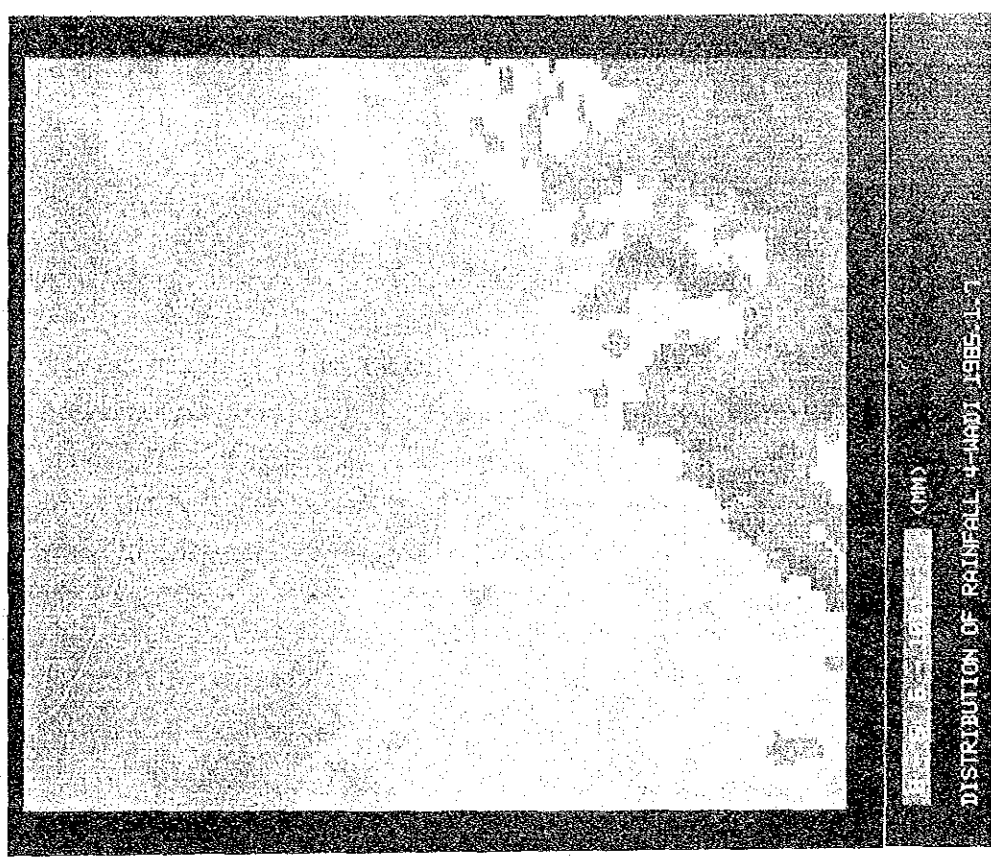
April 14, and August 9, 1983, and December 31, 1984

Data for these three days were collected for April 13, August 10 and December 29, respectively, as information around the day of rainfall. The amount of rainfall on these days were not used for the distribution analysis.

Fig. F-2-4 (3) Precipitation Distribution Image (3/3)



(a) Apr. 13, 1983



(b) Jan. 7, 1985

CHAPTER 3 NOAA IMAGE ANALYSIS ON SOIL MOISTURE

3.1 Objectives and Methods

3.1.1 Objectives

NOAA Satellite mounts an AVHRR (Advanced Very High Resolution Radiometer) sensor which detects radiant energy of five different wave bands. The satellite passes over Oman twice a day (day/night). Bands 1 and 2 are assigned to visible and near-infrared wave lengths, and bands 3, 4 and 5 are assigned to thermal wave lengths.

The first purpose of the NOAA image analysis is to investigate the detectability of soil moisture. The second purpose is to make a trial for estimation of the regional distribution of wet surface changing day by day after rainfall.

3.1.2 Method of Image Processing

Shown in Fig. F-3-1 is the procedure from the acquisition of NOAA CCT (Computer Compatible Tape) to the final image output.

Two kinds of final image outputs can be analytically obtained. The first is for visible/near-infrared bands (Bands 1 and 2), and the second is for infrared bands (Bands 3, 4 and 5).

(1) Visible/near-infrared bands

The visible and near infrared bands data are used for processing of daytime NOAA images. The reflection coefficient of both bands depends on the soil moisture content of ground surface and the principle of daytime image processing is based on this fact. The ratio (A_1/A_2) of two reflection coefficients (A_1, A_2) of bands 1 and 2 was adopted for the final image output.

(2) Thermal bands

The visible data of night-time NOAA images are not available. Therefore, the processing of night-time data is made only for the thermal band images. The principle of the processing is based on Planck's equation as follows:

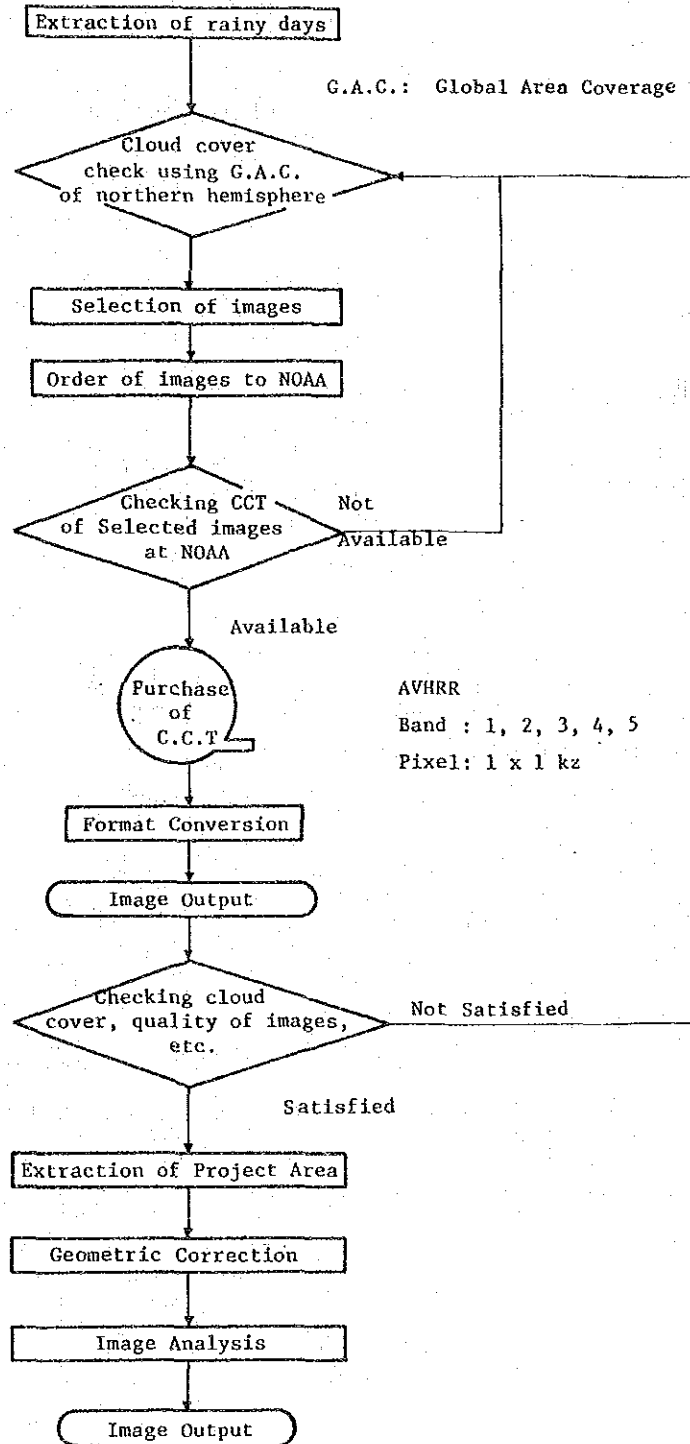
$$E_i = \epsilon_i \frac{C_1}{\lambda_i^5} \cdot \frac{1}{\frac{C_2}{e^{\lambda_i \cdot T}} - 1}$$

Where,

- E_i : emissive energy of band i
- ϵ_i : emissivity of band i
- C_1, C_2 : constant
- λ_i : wave length of band i
- T : absolute temperature

The emissivity depends on soil moisture content of ground surface. The value ($E_4^{\lambda_4}/E_5^{\lambda_5}$) corresponding to the ratio (ϵ_4/ϵ_5) of bands 4 and 5 was adopted for the final image output.

Fig. F-3-1 Flow Chart of NOAA Image Processing for Soil Moisture Analysis



3.2 Ground Truth Experiment

3.2.1 Condition and Method

For the purpose of determining analytical principles and the evaluation of final image output, the ground truth experiment is indispensable.

Four kinds of soil samples were collected and used for the experiment.

- 1) silt
- 2) sand
- 3) unconsolidated sand and gravel
- 4) semi-consolidated sand and gravel

Water was poured into the four samples above, artificially producing various water contents. The property of reflection and emission at the surface was observed and then analyzed.

The specification of the experiment is shown in Table F-3-1. The sensors are selected to correspond to the AVHRR of NOAA satellites. Three different incident angles (10° , 25° , 40°) of light angle are also taken into account in consideration of solar elevation. The calibration of the visible/near-infrared reflectometer is made by white board and water, and the calibration of the middle infrared and far infrared radiation thermometers are made by water.

3.2.2 Results of Experiment

The results on band width of middle and far infrared are exhibited in Figs. F-3-2 and F-3-3. No clear relation can be seen between ratio of emissivity and water content. The results on band width of visible (red) and near infrared are exhibited in Fig. F-3-4. A clear correlation can be seen between ratio of spectral reflectance and water content for all samples.

Table F-3-1 Specification of Ground Truth Experiment on Spectral Reflectance and Emissivity of Surface Soil Moisture

Sensor type	Visible	Middle infrared	Far infrared	Remarks
Wave length(λ)	0.6-0.7 μm 0.7-1.1 μm	2.0 μm ~5.2 μm	9 μm ~12 μm	<p>Object</p> <p>θ_2 : Incidence angle of Light source (10°, 25°, 40°)</p>
Incidence angle of Sensor (θ_1)	5°	15°	15°	
View angle(α)	1.1° X 9.1°	0.29°	1°	
Distance between sensor and object(L_1)	92cm	108cm	100cm	
Object area (S)	26.5cm ²	0.24cm ²	19.6cm ²	
Distance between light source and object(L_2)	80cm	80cm	80cm	
Illuminating power of light source (horizontal brightness)	170 candela (12V50W halogen lamp)	170 candela (12V50W halogen lamp)	170 candela (12V50W halogen lamp)	

Fig. F-3-2 Relation between Ratio of Emisivities and Soil Water Content

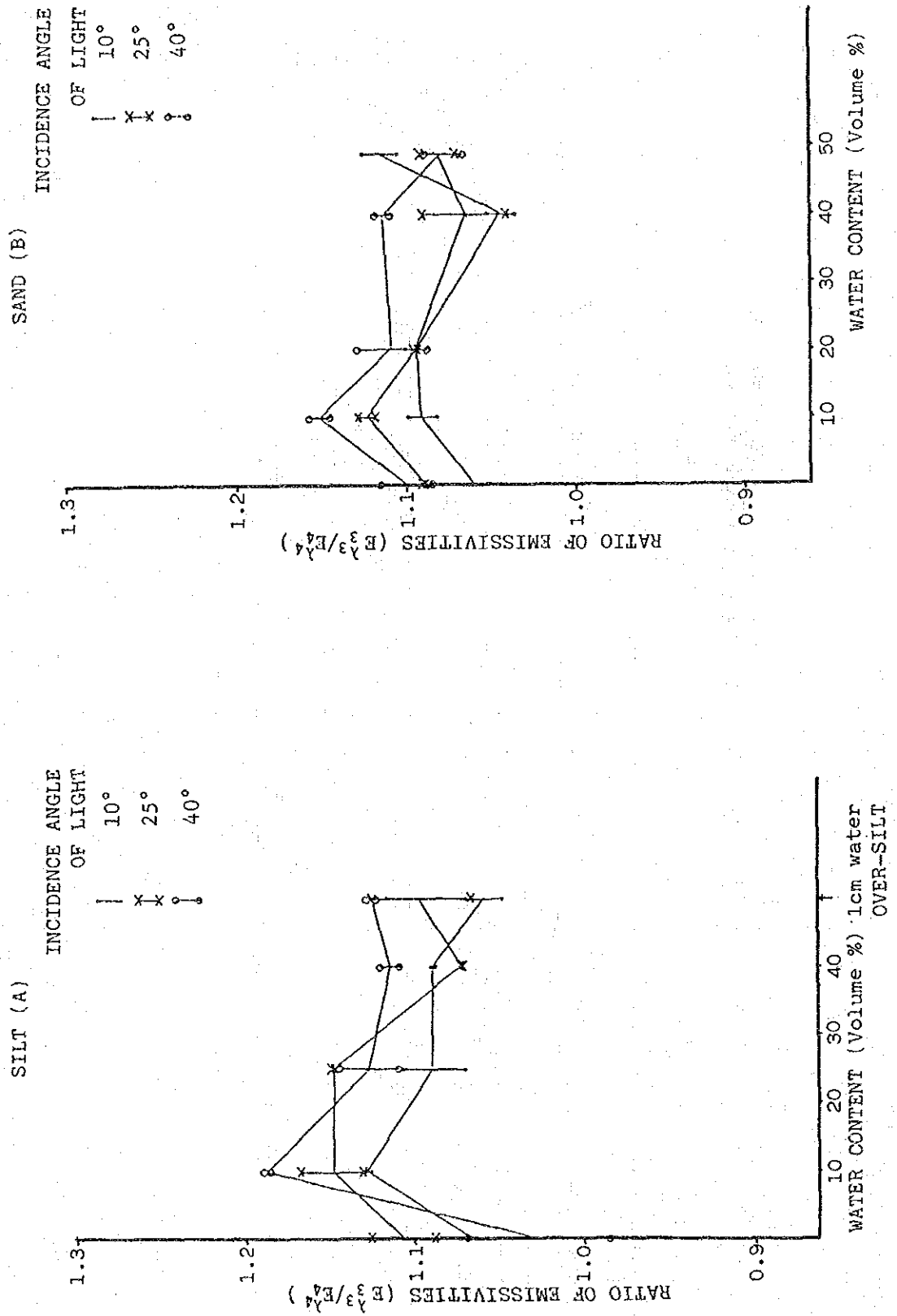


Fig. F-3-3 Relation between Ratio of Emisivities and Moisture Condition

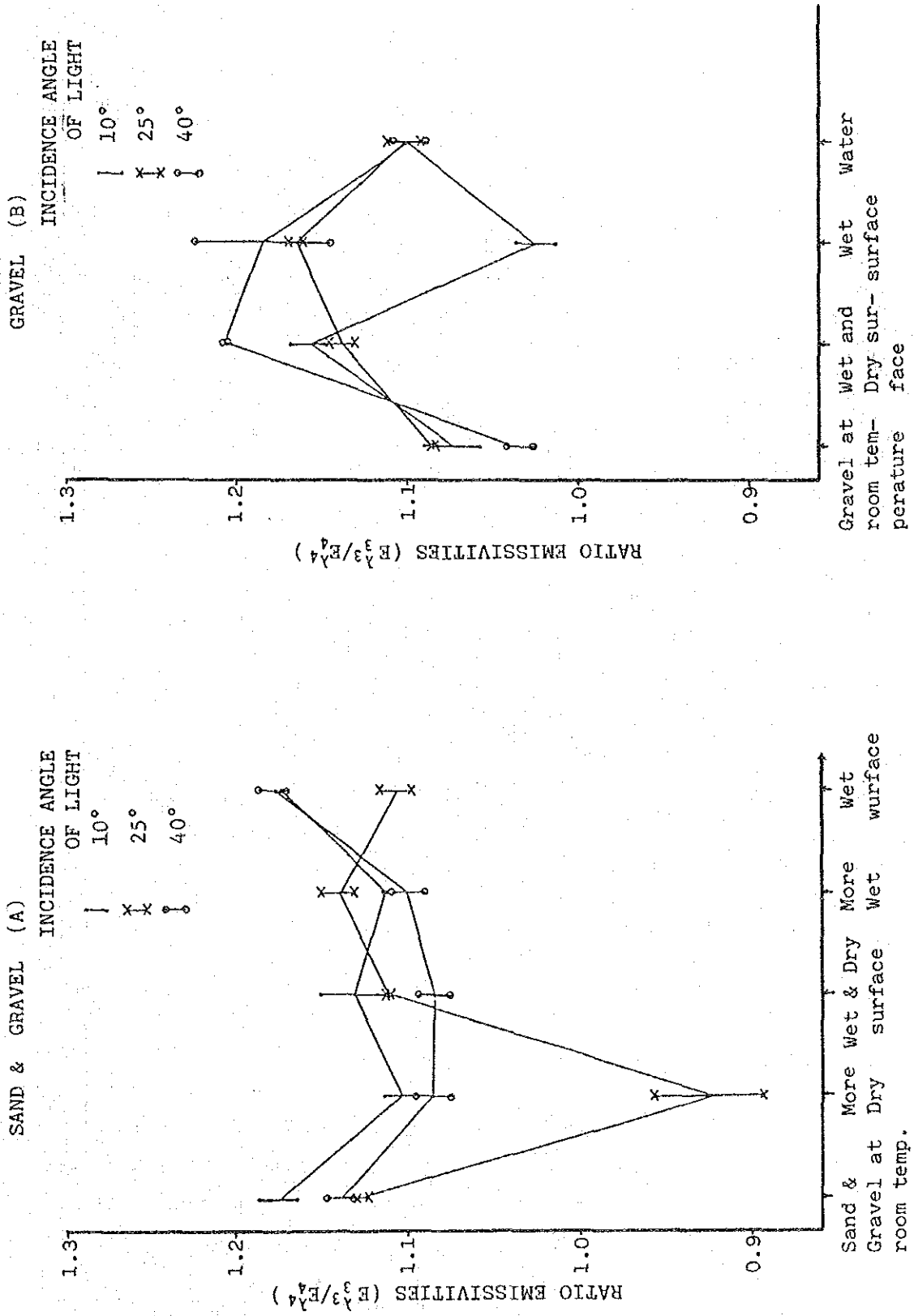
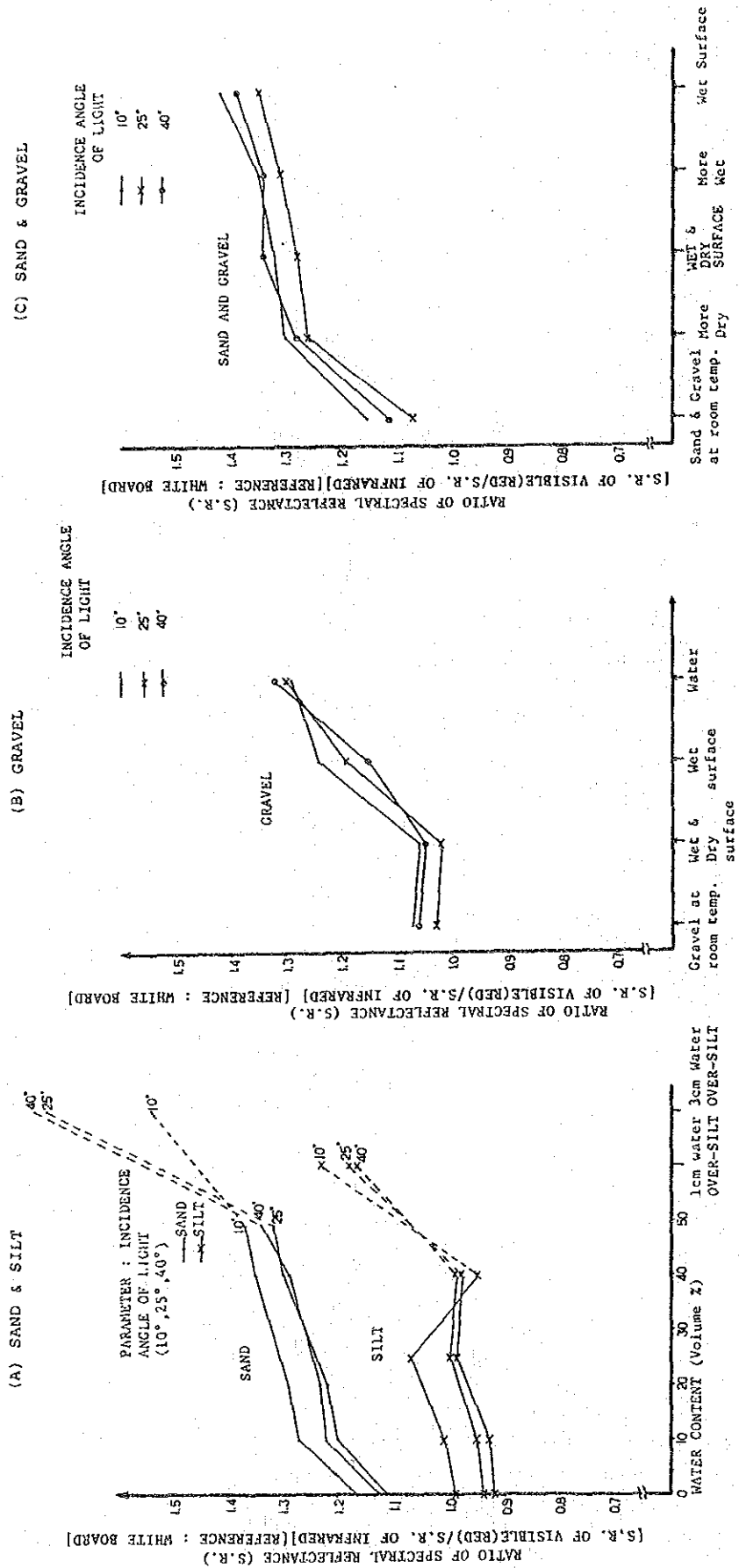


Fig. F-3-4 Relation between Ratio of Spectral Reflectance and Moisture Condition



3.3 Soil Moisture Distribution Analysis

3.3.1 Selection of NOAA Image for Processing

The selection of NOAA image for processing was done based on the following conditions:

- 1) The project area is not covered with cloud
- 2) The images are available for a period from a few days before rainfall to a few weeks after rainfall.
- 3) The series of images above are either daytime image or night-time images.

The images available and actually processed are listed in Table F-3-2. The number of images which satisfy the conditions above was unfortunately limited.

3.3.2 Processing of visible/near infrared images

For the rainfall during April 24 - May 4, 1981, the most NOAA CCTs were available among all the past rainfalls. The intensive processing was therefore done for that rainfall as mentioned below.

The comparison in albedo of sea area between Bands 1 and 2 is exhibited in Fig. F-3-5. Although the absolute value shows a great diversity, the ratio between them ($A1/A2$) is stable before and after rainfall. The ratio of land area, even after being normalized by the ratio of sea area, varies before and after rainfall at rain gauge sites as shown in Fig. F-3-6. The image ($A1/A2/SEA$) obtained for whole project area is shown in Fig. F-3-7.

The average ratio ($A1/A2/SEA$) between April 22 and 23 before rainfall was obtained on pixel by a pixel basis and is shown in Fig. F-3-8. This figure exhibits the reflection property of dry ground surface. Each of four images after rainfall in Fig. F-3-7 was subtracted from the standard image of dry surface (Fig. F-3-8) and subsequently-produced four subtraction images were then superimposed one by one. The resultant image produced is Fig. F-3-9, which illustrates the reduction of wet surface with time after rainfall.

3.3.3 Processing of Thermal Images

For the thermal bands the available night-time images were limited only for the rainfall on Feb. 26 - 29, 1982. Shown in Fig. F-3-10 are the three images before and after the rainfall using the ratio $(E_4^{\lambda_4}/E_5^{\lambda_5}/SEA)$ corresponding to the ratio of emissivity.

Table F-3-2(1) Daily Rainfall Amount at Conventional Gauge Sites, NOAA Image Availability and Weather Condition (Apr. 21-May. 23, 1981)

1982

DATE	M1	Khasun	Avabl.	Rustaq	Ravqaqn	Hayl	Al Ghozalifan Al Qufays	Haybl	Sabas	NOAA DATA		WEATHER
										AVAILABILITY	2:00 14:00	
2/14	16.0	-	26.0	7.0	8.0	-	38.0	-	-	A	A	C
15	-	-	-	10.0	-	-	-	-	-	A	A	FAIR
16	-	-	-	-	-	-	-	-	-	R	A	FAIR
17	-	-	-	-	-	-	26.0	-	-	A	A	PC
18	-	-	-	-	-	-	59.4	-	-	A	A	FAIR
19	-	-	-	-	-	-	-	-	-	A	A	C
20	-	-	-	-	-	-	-	-	-	PC	C	C
21	-	-	-	-	-	-	-	-	-	NA	NA	PC
22	2.0	-	-	7.2	20.0	-	2.3	-	-	R	NA	PC
23	70.0	51.3	56.0	47.3	46.0	-	35.0	4.0	-	A	A	C
24	1.0	-	-	-	25.0	-	-	16.0	-	P	A	C
25	36.0	-	-	-	10.0	-	1.5	20.0	-	R	A	FAIR
26	10.0	19.0	7.2	10.0	15.0	-	-	-	-	A	A	C
27	-	-	-	-	-	-	-	-	-	P	P	FAIR
28	-	-	-	-	-	-	-	-	-	P	P	FAIR
3/1	-	-	-	-	-	-	10.0	-	-	P	NA	FAIR
2	-	-	-	-	-	-	-	-	-	NA	NA	FAIR
3	-	-	-	-	-	-	-	-	-	R	NA	PC
4	0.0	-	-	-	-	-	-	-	-	A	P	FAIR
5	-	-	-	-	-	-	-	-	-	R	A	C
6	-	-	-	-	-	-	-	-	-	NA	NA	FAIR
7	5.0	-	-	-	-	-	-	-	-	NA	NA	FAIR
8	-	-	-	-	-	-	-	-	-	NA	NA	PC
9	-	-	-	-	-	-	-	-	-	NA	NA	FAIR
10	-	-	-	-	-	-	-	-	-	R	A	FAIR
11	4.0	-	-	10.5	2.0	-	2.7	-	-	A	A	FAIR
12	0.0	-	-	9.5	10.0	-	5.0	10.0	-	A	NA	FAIR
13	-	-	-	-	0.0	-	6.0	6.5	-	A	NA	FAIR
14	-	-	-	-	0.0	-	-	-	-	A	NA	FAIR
15	-	-	-	-	0.0	-	-	-	-	P	C	FAIR
16	-	-	-	-	-	-	-	-	-	A	NA	FAIR
17	-	-	-	-	-	-	-	-	-	NA	NA	FAIR
18	-	-	-	-	-	-	-	-	-	NA	NA	FAIR
19	-	-	-	-	-	-	-	-	-	NA	NA	FAIR
20	-	-	-	-	-	-	-	-	-	NA	NA	FAIR
21	-	-	-	-	-	-	-	-	-	NA	NA	FAIR
22	-	-	-	-	-	-	-	-	-	A	A	PC
23	-	-	-	-	-	-	-	-	-	A	A	FAIR
24	-	-	-	-	-	-	-	-	-	A	A	FAIR
25	-	-	-	-	-	-	-	-	-	NA	NA	FAIR
26	-	-	-	-	-	-	-	-	-	NA	NA	PC
27	-	-	-	-	-	-	-	-	-	A	A	PC
28	-	-	-	26.5	18.0	-	-	-	-	A	A	C
29	-	-	13.2	65.0	12.0	-	-	-	-	A	NA	C
30	-	48.0	-	-	3.0	-	-	-	-	A	NA	PC
31	-	-	-	-	-	-	-	-	-	A	NA	C

LEGEND
 A : Available
 NA : Not Available
 P : Data Processed
 R : Data Received
 PC : Partly Cloudy
 C : Cloudy

Table F-3-2 (2) Daily Rainfall Amount at Conventional Gauge Sites, NOAA Image Availability and Weather Condition (Feb. 14-28 and Mar. 1-31, 1982)

1981

DATE	Ali	Khatun	Avabi	Rustaq	Havqayn	Hayl	Al Ghozaifan	Al Qufays	Haybi	Seham	NOAA DATA AVAILABILITY		WEATHER CONDITION	
											7:00	19:00	7:00	19:00
4/21	-	-	-	-	-	-	-	-	-	-	A	A	FAIR	FAIR
22	-	-	-	-	-	-	-	-	-	-	P	A	FAIR	PC
23	-	-	-	-	-	-	-	-	-	-	P	A	FAIR	C
24	3.0	-	-	-	-	-	-	-	-	-	C	C	C	C
25	-	-	-	5.8	0.0	-	1.0	-	-	-	-	-	C	PC
26	-	-	-	(5.4)	0.0	-	-	-	2.0	-	A	A	FAIR	PC
27	-	-	-	-	0.0	-	5.2	2.2	-	-	A	A	FAIR	C
28	1.0	-	-	1.8 (0.8)	5.0	-	-	-	-	-	A	A	FAIR	PC
29	-	-	-	0.2 (0.2)	2.0	-	-	-	-	-	A	A	FAIR	FAIR
30	-	-	-	-	0.0	-	-	-	-	-	A	A	FAIR	FAIR
5/1	-	8.5	-	-	-	-	-	-	-	-	NA	NA	FAIR	PC
2	21.0	-	4.5	34.5 (7.0)	65.0	-	13.0	-	20.3	-	P	A	PC	FAIR
3	12.0	-	-	0.3 (22.6)	0.0	-	4.5	18.0	-	45.7	NA	P	PC	C
4	-	-	-	-	-	-	-	4.5	-	2.1	NA	P	PC	C
5	-	-	-	-	-	-	-	-	-	-	P	P	FAIR	FAIR
6	-	-	-	-	-	-	-	-	-	-	P	A	FAIR	FAIR
7	-	-	-	-	-	-	-	-	-	-	P	A	FAIR	FAIR
8	-	-	-	-	-	-	-	-	-	-	P	A	FAIR	FAIR
9	-	-	-	-	-	-	-	-	-	-	A	A	FAIR	FAIR
10	-	-	-	-	-	-	-	-	-	-	A	A	FAIR	FAIR
11	-	-	-	-	-	-	-	-	-	-	P	NA	FAIR	PC
12	-	-	3.2	-	-	-	-	-	-	-	NA	NA	FAIR	PC
13	-	-	-	-	-	-	-	-	-	-	NA	A	FAIR	FAIR
14	-	-	-	-	-	-	-	-	-	-	A	A	FAIR	FAIR
15	-	-	-	-	-	-	-	-	-	-	A	A	FAIR	FAIR
16	-	-	-	-	-	-	-	-	-	-	P	A	FAIR	FAIR
17	-	-	-	-	-	-	-	-	-	-	P	A	FAIR	FAIR
18	-	-	-	-	-	-	-	-	-	-	A	NA	FAIR	FAIR
19	-	-	-	-	-	-	-	-	-	-	A	NA	FAIR	FAIR
20	-	-	-	-	-	-	-	-	-	-	A	NA	FAIR	FAIR
21	-	-	-	-	-	-	-	-	-	-	A	NA	FAIR	FAIR
22	-	-	-	-	-	-	-	-	-	-	P	A	FAIR	FAIR
23	-	-	-	-	-	-	-	-	-	-	A	P	FAIR	FAIR

UNITS: MM

LEGEND
A : Available
NA : Not Available
P : Data Processed
R : Data Received
PC : Partly Cloudy
C : Cloudy

Table F-3-2 (3) Daily Rainfall Amount at Rain Gauge Sites Installed by JICA, NOAA Image Availability and Weather Condition (Aug. 1-24 and Sep. 1-24, 1983)

Unit : mm

DATE	MULADDAN MET. ST. IN RUWI																NOAA DATA	WEATHER										
	RA1	RA2	RA3	RA4	RA5	RG1	RG2	RG3	RG4	RG5	RF1	RF2	RF3	RF4	RF5	RK1			RK2	RK3	RK4	RK5	RK6	RM1	RM2	RM3	RM4	
8/1																												PC
8/2																												PC
8/3																												CC
8/4																												CC
8/5																												CC
8/6																												CC
8/7																												CC
8/8																												CC
8/9																												CC
8/10	15.0	43.5				1.5	7.0		37.0	36.5	53.0	19.0	4.5	21.0	7.5	6.0	37.5	25.5	17.5	40.0	4.0	1.5	11.5				CC	
8/11	5.0	6.0			5.0					0.5	1.0	0.5		0.2						32.0							CC	
8/12																												CC
8/13																												CC
8/14																												CC
8/15																												CC
8/16																												CC
8/17																												CC
8/18																												CC
8/19																												CC
8/20																												CC
8/21																												CC
8/22																												CC
8/23																												CC
8/24																												CC
9/1																												CC
9/2																												CC
9/3																												CC
9/4																												CC
9/5																												CC
9/6																												CC
9/7																												CC
9/8																												CC
9/9																												CC
9/10																												CC
9/11																												CC
9/12																												CC
9/13																												CC
9/14																												CC
9/15																												CC
9/16																												CC
9/17																												CC
9/18																												CC
9/19																												CC
9/20																												CC
9/21																												CC
9/22																												CC
9/23																												CC
9/24																												CC

LEGEND

RA1 : Saham
 RA2 : Al-Hay1
 RA3 : Haihi
 RA4 : Al-Qufeis
 RA5 : Al-Yuqbah

RG1 : Al-Suwaig
 RG2 : Al-Araq
 RG3 : Al-Kouqain
 RG4 : Daba'
 RG5 : Yiga'

RF1 : Al-Awg
 RF2 : Madruj
 RF3 : Al-Zammah
 RF4 : Sin Jamma
 RF5 : Al-Rustaq

RK1 : Khatm
 RK2 : Al-Habbi
 RK3 : Al-Hajar
 RK4 : Al-Hudsanah
 RK5 : Al-Ghubrah
 RK6 : Al-Khadrah

RM1 : Barke'
 RM2 : Sin Khatw
 RM3 : Afi
 RM4 : Ard Al-Habbil

A : Available
 NA : Not Available

P : Data Processed
 X : No Record

PC : Partly Cloudy
 C : Cloudy

Fig. F-3-5 Albedo (A1, A2) of Bands 1 and 2 of Sea Surface, Gulf of OMAN, and Albedo Ratio (A1/A2)

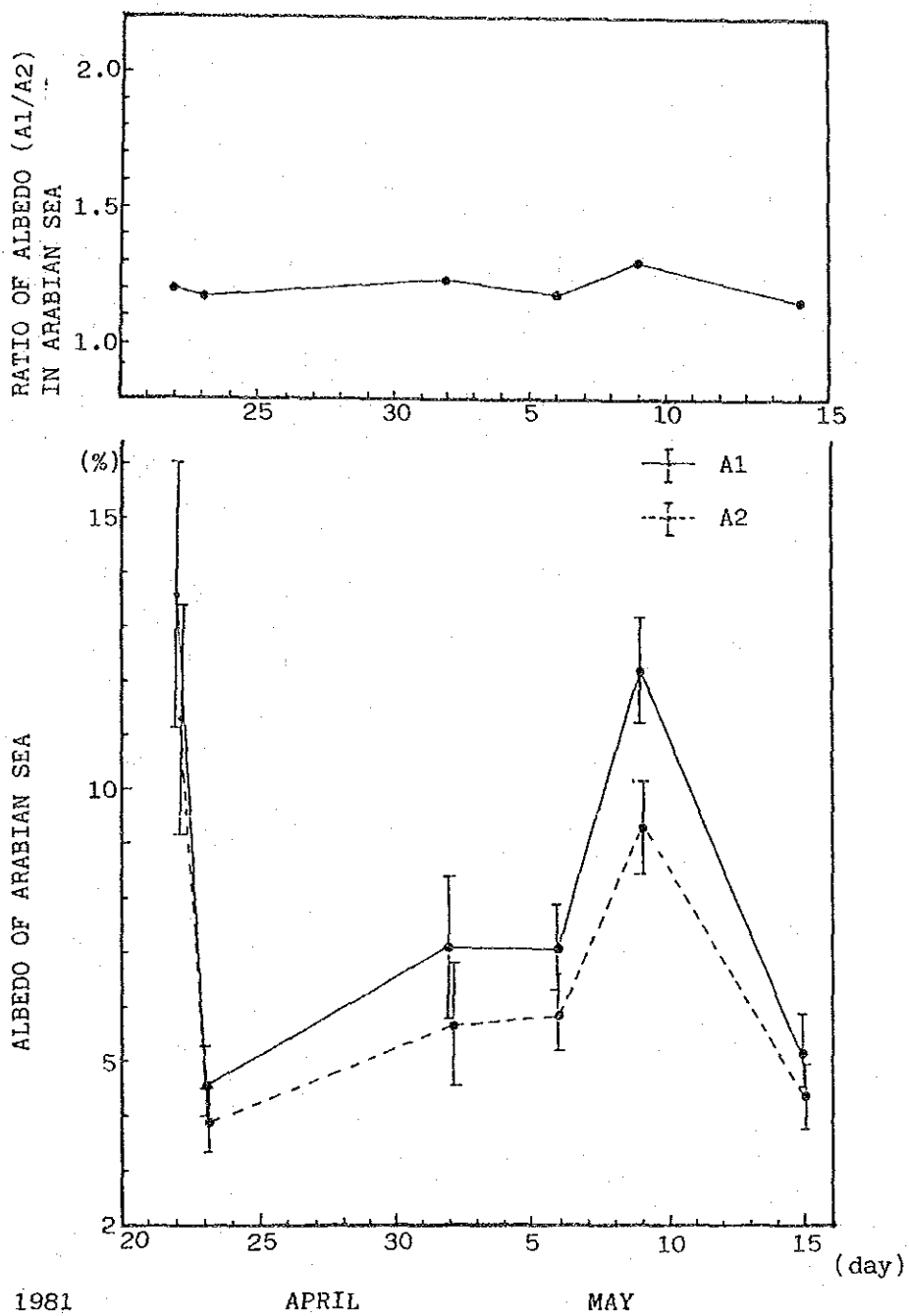


Fig. F-3-6 Change of Albedo Ratio ($A1/A2/SEA$) Normalized by Sea before and after Rainfall in Apr.-May, 1981 at Conventional Gauge Sites

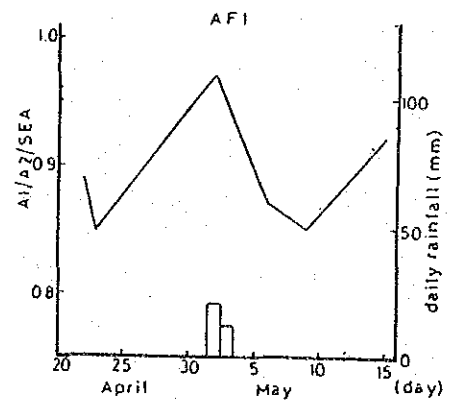
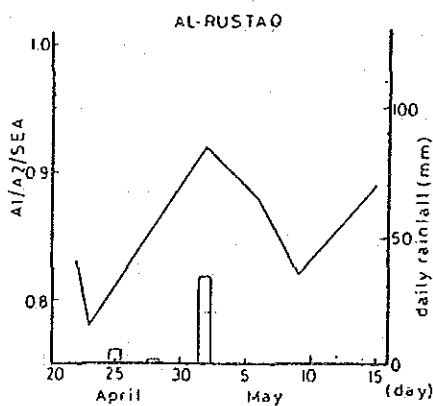
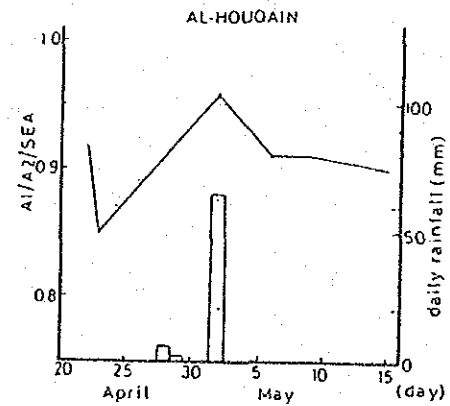
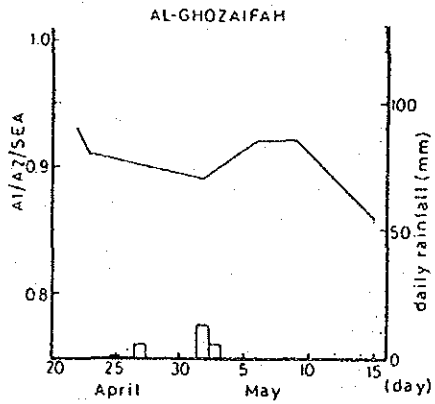
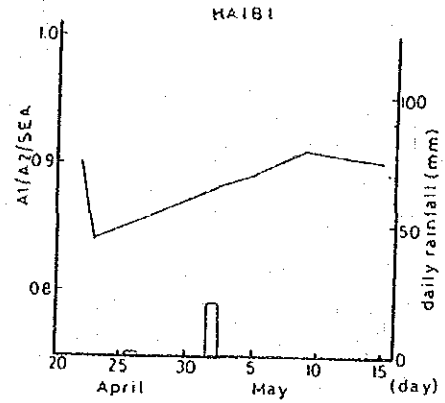
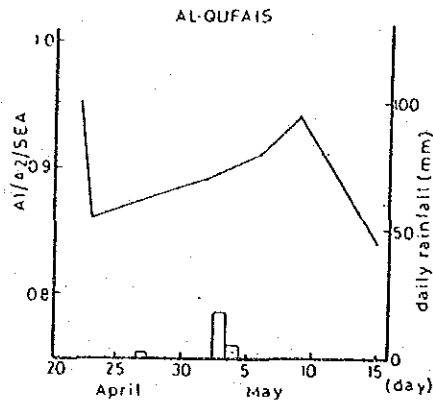
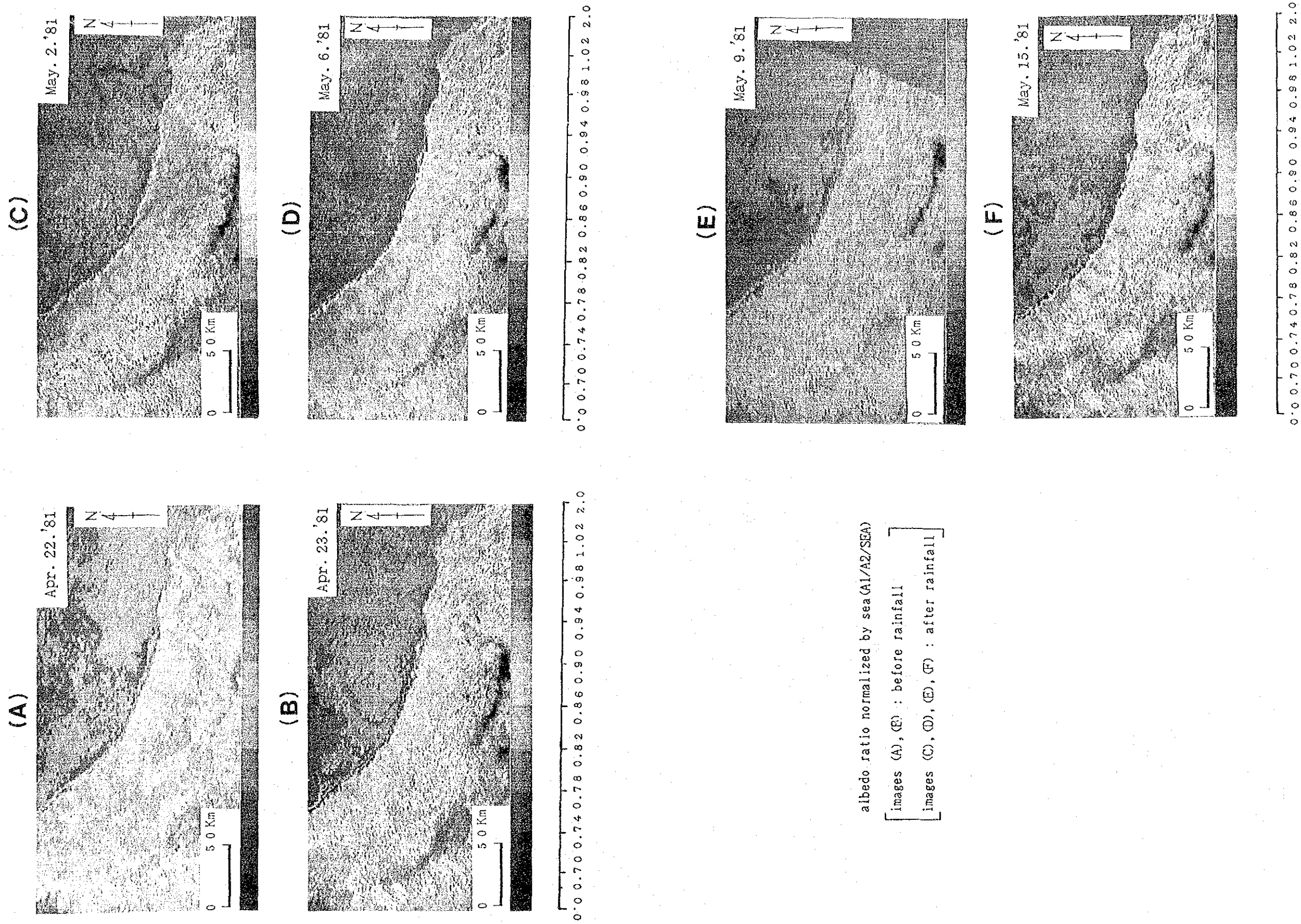


Fig. F-3-7 Processed NOAA Images Showing Distribution of Albedo Ratio Normalized by SEA (A1/A2/SEA)



albedo ratio normalized by sea (A1/A2/SEA)

[images (A), (E) : before rainfall
 [images (C), (D), (E), (F) : after rainfall]

Fig. F-3-8 Processed NOAA Image Showing Dry Surface Condition
(Average between Two Images of Apr. 22 and 23, 1981)

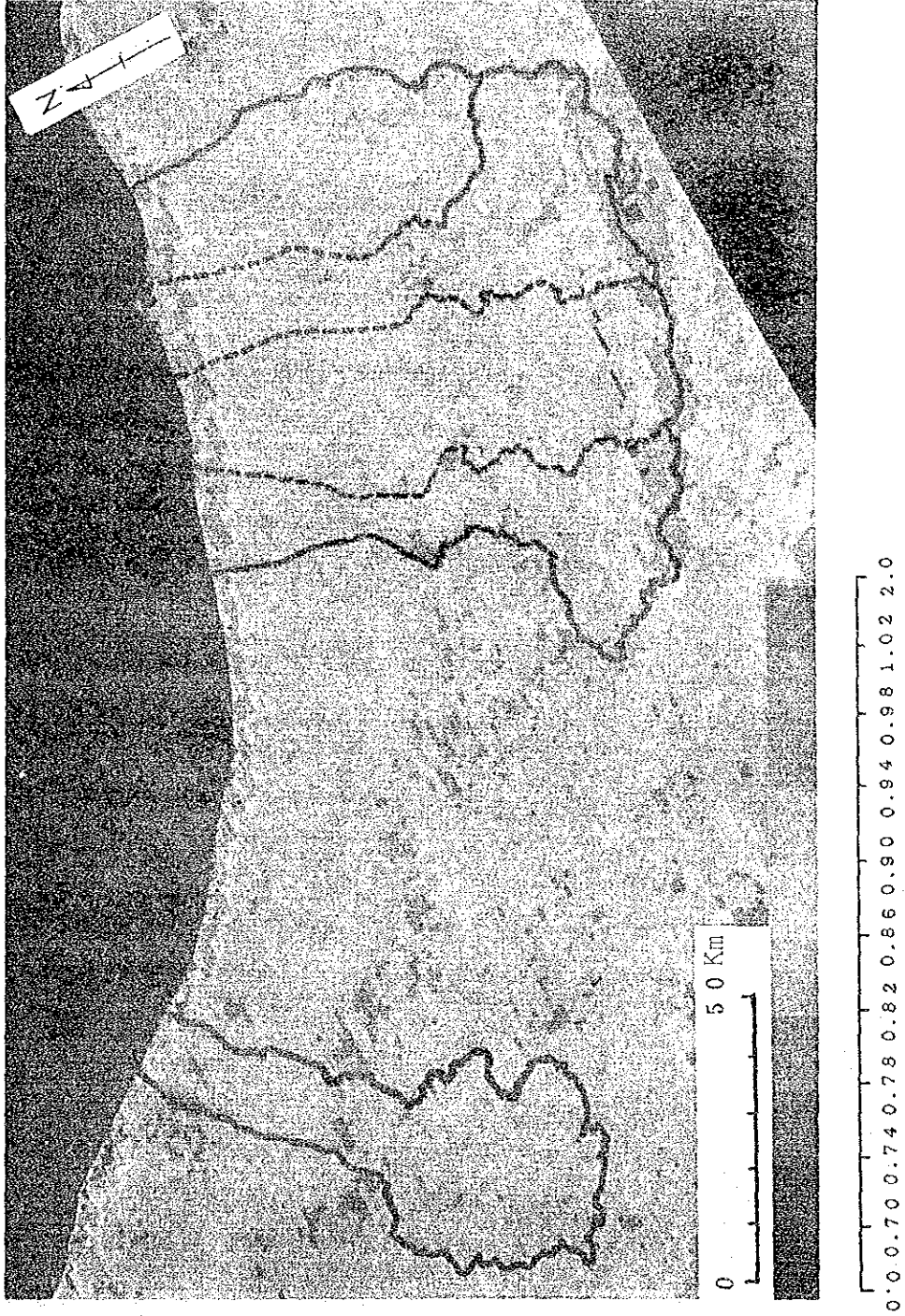
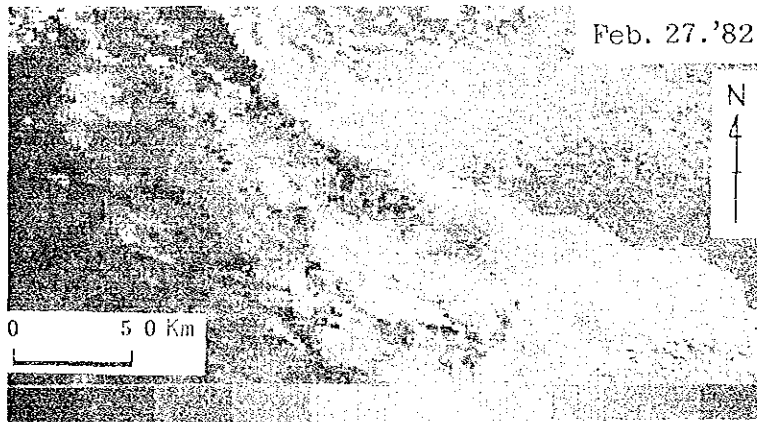
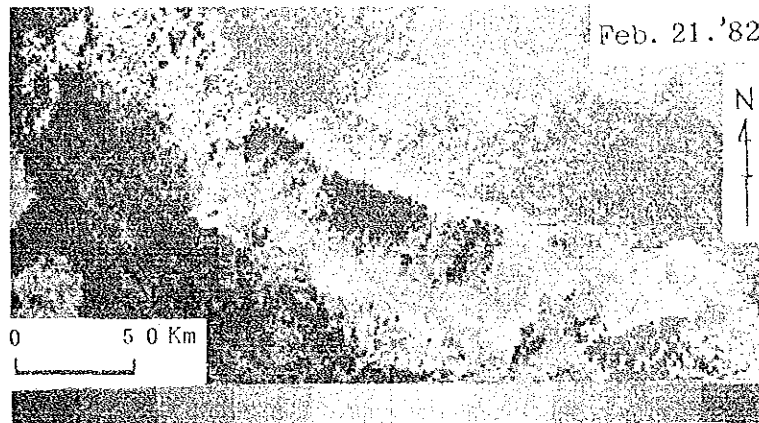


Fig. F-3-9 Processed NOAA Image Showing Retreat of Wet Surface after Rainfall



- Note : Black : Dehydrated before May 2nd, 1981
Red : Dehydrated between May 2nd and May 6th, 1981
Orange : Dehydrated between May 6th and May 9th, 1981
Blue : Dehydrated between May 9th and May 15th, 1981
Dark blue : Dehydrated after May 15th, 1981

Fig. F-3-10 Processed NOAA Images of Thermal Bands ($E_4^{\lambda 4}/E_5^{\lambda 5}/SEA$)



0 0.70 0.74 0.78 0.82 0.86 0.90 0.94 0.98 1.02 2.0

CHAPTER 4 CONCLUDING REMARKS

4.1 LANDSAT Analysis for Topographic, Geologic and Vegetation Distribution Survey

The ground surface resolution of LANDSAT is $100 \times 100 \text{ m}^2$ approx., and it is suitable for the detection of ground surface conditions in detail compared with NOAA. The LANDSAT image analyses focussed on the detection of topography, geology and vegetation.

The LANDSAT topographic and geologic analysis was useful for the identification of the boundary between lithofacies and for the extraction of large-scale fracture systems. It was also utilized for grasping the location and configuration of sand dunes.

Regarding vegetation, the analysis of three images of different years was carried out aiming at the extraction of the time-series change of land use. The analytical results were used for the estimation of land use area and then of water use in the hydrologic water balance analysis.

4.2 NOAA Rainfall Distribution Analysis

By means of NOAA images on rainy days, the analyses were carried out for the rainfall distribution.

On a rainy day, the cloud covers the ground surface, so that the NOAA image is of the cloud summit. Thermal band data were used, and a multiple regression equation was derived for each rainfall in consideration of the altitude. The analysis was not fully satisfactory because of the abnormal scarcity of rainy days during the project and lack of available NOAA CCT. However, this analysis lead to a way of estimation of rainfall distribution by means of NOAA images. The analytical method is best adapted to the estimation of regional distribution of annual rainfall etc. in the area where ground observation sites are scarce.

4.3 NOAA Image Analysis of Soil Moisture

Detection of surface soil moisture distribution after rainfall was carried out by means of NOAA image processing. The resolution of NOAA image is $1 \times 1 \text{ km}^2$ under the satellite trajectory which is worse than that of LANDSAT images. NOAA's advantage, however, is the provision of the image two times a day (day and night).

The digital images are preserved at National Oceanic and Atmospheric Administration, USA. As the volume of preservation increases year by year, the preservation in recent years decreases drastically for the area with less demand. Thus, the number of available images in the project area became very limited especially for those after the installation of new observation network. In addition, there was abnormal scarcity of rainy days in this period. The NOAA image processing was, therefore, obliged to focus on the rainfall before the project started.

The NOAA image processing for soil moisture has, thus, faced many unpredictable difficulties at the beginning of the project. However, the analysis has made notable achievements as listed below:

1. The detection of soil moisture by means of NOAA image processing had not been technically exploited at all. The methodological study done in this project threw light on the detection.
2. NOAA Satellite has five sensor bands assigned to visible/near infrared wave lengths and thermal wave lengths. The former daytime image was clarified to be more suitable for the detection of soil moisture.
3. The analyses of daytime images obtained before and after rainfall revealed the distribution of the soil moisture and its change with time.
4. The analytical results extracted the characteristic distribution features of soil moisture, which coincides with the topographic and geologic distributions.
5. The change of soil moisture with time is related to the infiltration capacity of soil. The analytical results were effectively utilized for the site selection of the soil infiltration experiments and also for the distribution map on infiltration capacity.

SUPPORTING REPORT G

HYDROLOGIC WATER BALANCE

TABLE OF CONTENTS

	<u>Page</u>
CHAPTER 1 TERMS OF HYDROLOGIC BALANCE AND THEIR COMPUTATION	
1.1 Rainfall (P_i)	G-1
1.2 Water use (W_i)	G-7
1.3 Groundwater Storage Change (ΔG_i).....	G-10
1.4 Surface Discharge to Lower Stream (D_i)	G-29
1.5 Subsurface Discharge to Lower Stream (I_i).....	G-29
CHAPTER 2 ESTIMATION OF THE HYDROLOGIC WATER BALANCE	
2.1 Equations of Hydrologic Water Balance	G-34
2.2 Quantitative Estimations of the Hydrologic Water Balance Terms	G-34
2.3 Results of Hydrologic Water Balance Estimation.....	G-38

LIST OF TABLES

		<u>Page</u>
G-1-1	Estimated Summer Rainfall	G-2
G-1-2	Estimated Winter Rainfall	G-3
G-1-3	Thiessen Polygon Distribution for Rain Gauge	G-5
G-1-4	Estimated Results of Annual Rainfall	G-6
G-1-5	Estimated Unit Water Consumption	G-7
G-1-6	Estimated Cropping Area	G-8
G-1-7	Water Use at Each Basin	G-9
G-1-8	Correlation Coefficient of Water Level	G-15
G-1-9	Thiessen Polygon Distribution for Observation Well	G-25
G-1-10	Estimated Results of Annual Groundwater Storage Change	G-28
G-2-1	Terms of the Hydrologic Cycle	G-30
G-2-2	Estimated Results of Annual Evapotranspiration of Soil Moisture	G-36
G-2-3	Wadi-bed Area Distreibution-Bi	G-37
G-2-4	Estimated Evapotranspiration from Wadi Bed	G-37
	(for 4 wadis, from Wadi Bani Ghafir to Wadi Al-Ma'awil)-Ei	
G-2-5	Estimated Evapotranspiration from Wadi Bed	G-37
G-2-6	Results of Estimated Hydrologic Water Balance	G-39

LIST OF FIGURES

		<u>Page</u>
G-1-1	Thiessen Polygons for Annual Rainfall Estimation	G-4
G-1-2	Thiessen Polygon Distribution for Observation Well.....	G-11
G-1-3	Computation Procedure of Groundwater Storage Change Estimation.....	G-12
G-2-1	Schematic Diagram of Hydrologic Balance Model	G-31
G-2-2	Schematic Diagram of Hydrologic Balance Terms	G-32
G-2-3	Conventional Assumptions for Hydrologic Water Balance Estimation	G-33
G-2-4(1)	Flow Diagram Showing the Estimated Results of Hydrologic Balance (Wadi Al-Ahin)	G-40
G-2-4(2)	"	
	(Wadi Bani Ghafir).....	G-41
G-2-4(3)	"	
	(Wadi Al-Fara')	G-42
G-2-4(4)	"	
	(Wadi Bani Kharus)	G-43
G-2-4(5)	"	
	(Wadi Al-Ma'awil).....	G-44

CHAPTER I TERMS OF HYDROLOGIC BALANCE AND THEIR COMPUTATION

Some water balance terms are presented in the Main Report. Hereafter their computation methods shall be explained of their backgrounds.

1.1 Rainfall (Pi)

In order to obtain the average annual rainfall of the project area, daily rainfalls, from January 1977 to July 1983, have been estimated depending on the previously observed rainfall data. Its method is explained in Supporting Report B 4.3.3. The number of the sites for the estimation, are 26 sites, which had started the observation by Aug. 1983. Table G-1-1 and Table G-1-2 show rainfall summations. In order to determine the rainfall volume, Thiessen method was adopted for the calculation. Fig. G-1-1 shows the Thiessen Polygon and Table G-1-3, presents the polygon area of each wadi basin. The downstream area between coastal wadi gauges and seashore was regarded as negligible in the estimation. In Table G-1-4 the rainfall volume is expressed in MCM/year unit.

Table G-1-1 Estimated Summer Rainfall

(mm/season)

Rain-gauge	1976 (Oct.-Dec.)	1977	1978	1979	1980	1981	1982	1983	1984	1985 (Jan.-May)	Mean
RA 1	15.2	120.2	59.9	116.8	1.2	49.4	117.1	76.9	26.0	0.5	64.8
2	25.9	104.4	43.1	89.5	34.4	63.1	152.4	142.0	4.0	0.0	73.2
3	47.2	146.3	71.3	71.4	28.3	75.8	236.0	102.5	4.5	10.5	88.2
4	31.2	114.2	46.6	67.5	25.0	31.2	193.8	128.6	1.5	0.0	71.1
5	58.9	172.7	75.6	110.0	37.1	63.9	281.2	163.1	3.5	2.5	107.6
RG 1	9.8	94.2	37.8	82.3	4.4	62.2	146.4	86.3	32.5	0.0	61.8
2	41.2	168.7	30.4	107.3	64.1	68.5	230.4	102.9	18.5	2.0	92.7
3	71.1	240.1	22.0	130.0	122.0	76.0	314.0	120.0	3.5	5.5	122.7
4	55.2	179.6	73.6	90.3	68.1	95.6	345.4	110.2	21.0	5.0	116.0
5	56.8	182.4	72.4	94.0	72.5	96.7	357.7	103.1	3.5	3.0	115.8
RF 1	58.5	191.3	73.6	98.1	82.7	102.2	385.7	106.3	24.5	8.5	125.7
2	53.7	203.7	85.4	87.9	89.1	113.8	399.7	145.0	7.5	31.0	135.2
3	60.5	193.8	71.9	102.6	87.2	103.0	398.6	100.2	30.5	27.5	130.6
4	30.8	122.3	42.2	87.8	33.9	74.4	241.2	76.8	15.5	0.0	80.5
MF 1	13.6	94.3	33.9	75.8	11.8	66.8	172.8	85.8	9.0	1.5	62.8
MF 2	65.2	178.8	59.1	112.5	78.2	89.5	377.6	59.0	14.1	3.0	115.2
RK 1	8.6	198.4	93.2	94.5	17.2	101.2	289.8	118.8	8.0	4.5	103.8
2	47.2	188.9	72.4	99.2	68.3	100.3	364.9	96.2	16.5	4.5	117.6
3	55.8	199.2	75.5	100.7	87.2	107.4	403.3	110.1	2.5	31.5	130.4
4	37.1	210.5	89.8	86.7	77.6	119.2	391.7	150.8	14.5	17.5	132.8
5	25.1	199.3	87.4	83.6	54.1	111.9	344.6	138.0	5.0	4.0	117.0
6	24.7	233.5	106.4	79.6	78.7	136.1	402.8	198.2	19.0	30.0	145.4
RM 1	6.2	82.5	25.3	55.3	8.7	74.3	180.8	95.4	39.0	1.5	63.2
2	7.3	115.9	46.3	69.2	10.1	79.1	200.1	99.0	7.0	0.0	70.4
3	6.5	180.0	82.5	79.5	16.0	99.0	267.7	114.0	11.5	5.0	95.7
4	21.1	187.7	81.7	85.1	39.0	103.1	312.3	117.1	1.0	24.5	108.1

* The values before May 1983 are estimated, and the values after Oct. 1983 are observed.

Table G-1-2 Estimated Winter Rainfall

	1976	1977	1978	1979	1980	1981	1982	1983	1984	1985 (June-July)	Mean (1976-1984)
RA 1	0.0	0.0	0.0	0.0	0.0	0.0	0.0	0.0	0.0	0.0	0.0
2	1.1	22.2	5.5	11.0	3.7	0.5	10.3	20.0	3.0	0.0	8.6
3	17.9	12.9	18.1	9.1	22.6	3.6	16.7	64.0	31.5	1.0	21.8
4	44.9	13.4	62.2	32.1	19.9	26.4	11.2	8.9	13.0	0.0	25.8
5	52.9	20.1	56.6	20.4	28.7	19.8	29.9	18.0	37.0	17.0	31.5
RG 1	0.0	0.0	0.0	0.0	0.0	0.0	0.0	1.5	0.0	0.0	0.2
2	0.0	0.0	0.0	0.0	0.0	0.0	0.0	7.0	0.0	0.0	0.8
3	8.9	7.4	0.5	1.2	10.2	0.0	0.5	16.5	2.5	0.0	5.3
4	65.2	11.0	54.9	20.5	13.2	5.5	5.4	62.0	19.0	0.0	28.5
5	46.0	13.9	64.7	26.0	32.8	16.9	25.3	48.5	19.0	27.0	32.6
RF 1	27.4	32.1	49.2	7.7	21.4	1.5	12.8	101.5	34.0	9.5	32.0
2	41.6	41.5	74.9	36.4	73.8	38.3	76.6	94.5	113.5	42.0	65.7
3	45.3	11.7	25.2	12.4	30.6	19.9	8.6	60.0	20.5	11.5	26.1
4	0.0	0.0	0.0	0.0	0.0	0.0	0.0	4.5	0.0	0.0	0.5
MF 1	0.0	0.0	0.0	0.0	0.0	0.0	0.0	6.5	0.0	0.0	0.7
2	42.1	3.8	16.4	15.4	17.7	0.5	3.0	58.6	5.0	1.5	18.1
RK 1	13.3	0.0	9.4	0.0	0.0	0.0	0.0	9.5	20.5	0.0	5.9
2	29.9	6.9	20.8	11.2	13.7	22.9	24.5	14.0	51.0	21.0	21.7
3	57.0	36.9	28.0	22.0	62.8	11.9	14.7	51.5	82.5	11.0	40.8
4	48.9	71.9	75.6	20.3	47.5	59.1	11.0	62.5	48.0	42.0	49.4
5	29.7	31.3	17.0	31.4	5.6	49.6	18.4	55.0	8.5	0.5	27.4
6	38.9	100.8	69.7	56.8	29.7	21.9	16.4	123.5	59.5	52.0	57.5
RM 1	0.0	0.0	0.0	0.0	0.0	0.0	0.0	4.0	0.0	0.0	0.4
2	0.0	0.0	0.0	0.0	0.0	0.0	0.0	1.5	0.0	0.0	0.2
3	0.0	0.0	4.4	0.0	0.0	0.0	0.0	11.5	0.0	0.0	1.8
4		12.2	1.6	5.1	1.1	1.0	12.3	13.0	7.2	0.0	0.0

* The values before 1982 are estimated, and the values after 1983 are observed.



Table G-1-3 Thiessen Polygon Distribution for Rain Gauge

(Km²)

	Wadi Ahin		Wadi Bani Ghafir		Wadi Al-Fara'		Wadi Bani Kharus		Wadi Al-Ma'awil	
Related Rain Gauge Sites	RA1	L 169.033	MF1	L 23.784	MF1	L 259.393	RM1	L 0.813	RM1	L 227.759
	RA2	L 185.053	RG1	L 104.331	RM2	L 8.560	RM2	L 210.469	RM2	L 116.712
	RA3	U 80.099	RG3	L 6.895	RG2	L 74.752	MF1	L 33.553	RM3	L 179.512
	RA4	U 152.042	RG3	U 149.901	RF4	L 314.735	RK1	L 139.194	RM3	U 181.953
	RA5	U 235.733	RF5	U 8.095	RF4	U 38.620	RK1	U 47.686	RM4	U 158.416
	-	U 296.803	RF1	U 14.690	RG3	L 20.505	RF4	L 19.115	RK1	L 49.615
	-	-	RF2	U 45.900	RG3	U 85.900	RF4	U 2.542	RK1	U 12.404
	-	-	RG5	U 274.818	RF5	U 212.710	RM4	73.715	RK5	U 73.250
	-	-	RG4	U 156.197	RK1	U 8.062	RK2	U 172.239	-	-
	-	-	RG2	L 146.703	RK2	U 99.238	RK5	U 176.713	-	-
-	-	-	-	RK3	U 18.713	RK6	U 102.286	-	-	
-	-	-	-	RF3	U 146.219	RK4	U 146.820	-	-	
-	-	-	-	RF1	U 140.645	RK3	U 120.791	-	-	
-	-	-	-	RF2	U 75.946	-	-	-	-	
-	-	-	-	RG5	U 15.328	-	-	-	-	
Total*	U	764.677	U	649.601	U	841.481	U	842.792	U	426.023
	L	354.086	L	281.713	L	677.945	L	403.144	L	573.598
	T	1.118.763	T	931.314	T	1.519.426	T	1.245.936	T	999.621

Note: Downstream area from coastal highway to seashore is neglected for water balance calculation.

* U; Mountain area for water balance (Upper stream)

L; Coastal area for water balance (Lower stream)

T; Total of Upper & Lower stream

Table G-1-4 Estimated Results of Annual Rainfall

W. Ahin (MCM/Year)

	77	78	79	80	81	82	83	84	Average
Upper	121.6	81.4	82.5	40.9	55.6	192.1	128.7	21.4	90.5
Lower	43.7	19.1	38.3	7.2	20.1	49.8	42.9	5.6	28.3
Basin	165.3	100.5	120.8	48.1	75.7	241.9	171.6	27.0	118.9

W.B.Ghafir

	77	78	79	80	81	82	83	84	Average
Upper	137.0	70.8	78.2	71.2	67.8	238.0	107.1	19.2	98.7
Lower	38.5	9.3	27.0	11.0	18.3	55.3	28.5	6.4	24.3
Basin	175.5	80.1	105.2	82.2	86.1	293.3	135.6	25.6	123.0

W. Al-Fara (MCM/Year)

	77	78	79	80	81	82	83	84	Average
Upper	172.0	77.4	98.8	90.0	89.8	323.7	129.1	37.8	127.3
Lower	82.4	25.2	58.6	21.3	47.9	146.0	61.8	8.8	56.5
Basin	254.4	102.6	157.4	111.3	137.7	469.8	190.9	46.6	183.8

W.B.Kharus (MCM/Year)

	77	78	79	80	81	82	83	84	Average
Upper	201.6	100.6	94.9	76.2	119.9	322.0	149.9	42.9	138.5
Lower	57.8	26.0	32.0	5.6	34.5	93.0	43.7	6.1	37.3
Basin	259.4	126.6	126.9	81.8	154.4	415.0	193.6	49.0	175.8

W. Al-Ma'awil (MCM/Year)

	77	78	79	80	81	82	83	84	Average
Upper	82.0	38.4	37.7	13.9	49.4	130.4	58.7	3.7	51.8
Lower	75.4	31.9	39.6	6.9	49.0	126.9	63.3	13.2	50.8
Basin	157.5	70.2	77.4	20.4	98.4	257.3	122.0	16.9	102.6

1.2 Water use (Wi)

Observed water use amounts are presented in Main Report 4.6 and Supporting Report E. In this survey observation was done in terms of in-take water volume itself so that unit water consumption for water balance were assumed like in Table G-1-5.

Unit water consumption for Upper stream (mountain area), defined in 5.1 of the Main Report, is assumed 3,000mm/year and 100% cropping ratio.

For the Lower stream (coastal area), also defined in the Main Report, the value would be 2,258mm/year and 75% cropping ratio.

Cropping area was determined as following.

The data of Gibb(1976) was adopted as the cropping area of 1976. Present cropping area was derived from the survey of this project and the value of each years were estimated by interporation. Table G-1-6 shows the cropping area and Table G-1-7 presents the estimation of water use volume in each wadi basin.

Table G-1-5 Estimated Unit Water Consumption

	Unit Water Consumption
Upper Stream (Mountain Area)	3,000 mm/year ^{1/}
Lower Stream (Coastal Area)	2,258 mm/year ^{2/}

^{1/} Unit water consumption in upper stream was estimated 3000mm/year based on the observed value 3108mm/year (1984/1985).
(cf. Main Report 4.6)

^{2/} Unit water consumption in lower stream was defined as 2258mm/year.

Table G-1-6 Estimated Cropping Area

W. Ahin *1 *2 (ha)

	76	77	78	79	80	81	82	83	84	Average
Upper	(73.0)	73.0	73.0	73.0	73.0	73.0	73.0	73.0	73.0	73.0
Lower	(326.0)	356.6	387.1	417.7	448.3	478.9	509.4	540.0	540.0	49.8
Basin	(399.0)	429.6	460.1	490.7	521.3	551.9	582.4	613.0	613.0	532.8

W.B. Ghafir (ha)

	76	77	78	79	80	81	82	83	84	Average
Upper	(295.7)	296.0	296.4	296.7	297.0	297.3	297.6	298.0	298.0	297.1
Lower	(1509.0)	1554.9	1600.7	1646.6	1692.4	1738.3	1784.1	1830.0	1830.0	1709.6
Basin	(1804.7)	1850.9	1897.4	1943.3	1989.4	2035.6	2081.7	2128.0	2128.0	2006.7

W. Al-Fara' (ha)

	76	77	78	79	80	81	82	83	84	Average
Upper	(754.5)	802.3	850.1	897.9	945.6	993.4	1041.2	1084.0	1084.0	963.6
Lower	(1507.0)	1531.7	1556.4	1581.1	1606.9	1630.6	1655.3	1680.0	1680.0	1615.3
Basin	(2361.5)	2334.0	2406.5	2479.0	2552.5	2624.0	2696.5	2764.0	2764.0	2578.9

W.B.Kharus (ha)

	76	77	78	79	80	81	82	83	84	Average
Upper	(381.4)	365.3	349.3	333.2	317.2	301.1	285.1	269.0	269.0	311.2
Lower	(834.0)	920.6	1007.1	1093.7	1180.3	1266.9	1353.4	1440.0	1440.0	1212.8
Basin	(1215.4)	1285.9	1356.4	1426.9	1497.5	1568.0	1638.5	1709.0	1709.0	1524.0

W. Al-Ma'awi (ha)

	76	77	78	79	80	81	82	83	84	Average
Upper	(499.9)	528.6	557.4	586.1	614.8	643.5	672.3	701.0	701.0	625.6
Lower	(1573.0)	1595.4	1677.9	1760.3	1842.7	1925.1	2007.6	2090.0	2090.0	1873.6
Basin	(2072.9)	2124.0	2235.3	2346.4	2457.5	2568.6	2679.9	2791.0	2791.0	2499.2

- *1) Cropping Area in 1976 from GIBB (1976).
- *2) Cf. Supporting E
- *3) Average Cropping Area (from 1977 to 1984).

Table G-1-7 Water Use at Each Basin

(MCW/YEAR)

	Wadi Ahin	Wadi Bani Ghafir	Wadi Al-Fara'	Wadi Bani Kharus	Wadi Al-Ma'awil	Total
Upper *1 Stream	2.2	8.9	28.9	9.3	18.8	68.1
Lower *2 Stream	7.8	29.0	27.4	20.5	31.7	116.4
TOTAL	10.0	37.9	56.3	29.8	50.5	184.5

*1) Water use was estimated as the unit water consumption of 3,000mm/year cropping ratio is 100%.

*2) Cropping ratio is 75%. Unit water consumption is 2,258mm/year.